

Title	Origin and passivation of fixed charge in atomic layer deposited aluminum oxide gate insulators on chemically treated InGaAs substrates
Authors	Shin, Byungha;Weber, Justin R.;Long, Rathnait D.;Hurley, Paul K.;Van de Walle, Chris G.;McIntyre, Paul C.
Publication date	2010
Original Citation	Shin, B., Weber, J. R., Long, R. D., Hurley, P. K., Walle, C. G. V. d. and McIntyre, P. C. (2010) 'Origin and passivation of fixed charge in atomic layer deposited aluminum oxide gate insulators on chemically treated InGaAs substrates', Applied Physics Letters, 96(15), pp. 152908. doi: 10.1063/1.3399776
Type of publication	Article (peer-reviewed)
Link to publisher's version	http://aip.scitation.org/doi/abs/10.1063/1.3399776 - 10.1063/1.3399776
Rights	© 2010 American Institute of Physics.This article may be downloaded for personal use only. Any other use requires prior permission of the author and AIP Publishing. The following article appeared in Shin, B., Weber, J. R., Long, R. D., Hurley, P. K., Walle, C. G. V. d. and McIntyre, P. C. (2010) 'Origin and passivation of fixed charge in atomic layer deposited aluminum oxide gate insulators on chemically treated InGaAs substrates', Applied Physics Letters, 96(15), pp. 152908 and may be found at http://aip.scitation.org/doi/abs/10.1063/1.3430061
Download date	2024-05-07 03:31:23
Item downloaded from	https://hdl.handle.net/10468/4343



UCC

University College Cork, Ireland
Coláiste na hOllscoile Corcaigh

Origin and passivation of fixed charge in atomic layer deposited aluminum oxide gate insulators on chemically treated InGaAs substrates

Byungha Shin¹, Justin R. Weber, Rathnait D. Long, Paul K. Hurley, Chris G. Van de Walle, and Paul C. McIntyre

Citation: *Appl. Phys. Lett.* **96**, 152908 (2010); doi: 10.1063/1.3399776

View online: <http://dx.doi.org/10.1063/1.3399776>

View Table of Contents: <http://aip.scitation.org/toc/apl/96/15>

Published by the [American Institute of Physics](#)

Articles you may be interested in

[Controlling the fixed charge and passivation properties of Si\(100\)/Al₂O₃ interfaces using ultrathin SiO₂ interlayers synthesized by atomic layer deposition](#)

Journal of Applied Physics **110**, 093715 (2011); 10.1063/1.3658246

[Presence and origin of interface charges at atomic-layer deposited Al₂O₃/III-nitride heterojunctions](#)

Applied Physics Letters **99**, 193504 (2011); 10.1063/1.3658450

[O₃-sourced atomic layer deposition of high quality Al₂O₃ gate dielectric for normally-off GaN metal-insulator-semiconductor high-electron-mobility transistors](#)

Applied Physics Letters **106**, 033507 (2015); 10.1063/1.4906601

[High- \$\kappa\$ gate dielectrics: Current status and materials properties considerations](#)

Journal of Applied Physics **89**, 5243 (2001); 10.1063/1.1361065

[Manipulating the negative fixed charge density at the c-Si/Al₂O₃ interface](#)

Applied Physics Letters **104**, 091604 (2014); 10.1063/1.4867652

[Interface charge engineering at atomic layer deposited dielectric/III-nitride interfaces](#)

Applied Physics Letters **102**, 072105 (2013); 10.1063/1.4793483



Origin and passivation of fixed charge in atomic layer deposited aluminum oxide gate insulators on chemically treated InGaAs substrates

Byungha Shin,^{1,a)} Justin R. Weber,² Rathnait D. Long,^{1,3} Paul K. Hurley,³ Chris G. Van de Walle,² and Paul C. McIntyre¹

¹Department of Materials Science and Engineering, Stanford University, Stanford, California 94305, USA

²Department of Materials, University of California, Santa Barbara, California 93106, USA

³Tyndall National Institute, University College Cork, Lee Maltings, Prospect Row, Cork, Ireland

(Received 23 September 2009; accepted 23 March 2010; published online 15 April 2010)

We report experimental and theoretical studies of defects producing fixed charge within Al₂O₃ layers grown by atomic layer deposition (ALD) on In_{0.53}Ga_{0.47}As(001) substrates and the effects of hydrogen passivation of these defects. Capacitance-voltage measurements of Pt/ALD-Al₂O₃/n-In_{0.53}Ga_{0.47}As suggested the presence of positive bulk fixed charge and negative interfacial fixed charge within ALD-Al₂O₃. We identified oxygen and aluminum dangling bonds (DBs) as the origin of the fixed charge. First-principles calculations predicted possible passivation of both O and Al DBs, which would neutralize fixed charge, and this prediction was confirmed experimentally; postmetallization forming gas anneal removed most of the fixed charge in ALD-Al₂O₃. © 2010 American Institute of Physics. [doi:10.1063/1.3399776]

In recent years, dimensional scaling of complementary metal-oxide-semiconductor (CMOS) devices has brought about serious interest in introducing high-mobility channel layers composed of III–V materials.¹ A longstanding problem for structures that include an oxide/III–V semiconductor interface has been the presence of interfacial defects that can trap charge during device operation. However, defects present in the *bulk* of a high permittivity (high-*k*) oxide layer that forms a relatively passive interface with III–V channel materials may be of equal importance because of their potential to increase gate leakage current, and to form fixed charge that will scatter carriers in the channel and alter the threshold voltage of the device.²

Many of the high-*k* dielectric materials investigated to replace SiO₂ in Si-channel MOS devices are grown as thin films with significant areal densities of fixed charge.³ However, the density of fixed charge either near the interface between ALD-Al₂O₃ and the channel or in the bulk of Al₂O₃ layers deposited on III–V materials such as InGaAs has not been studied carefully. In this paper, we report experimental and theoretical studies of defects producing fixed charge⁴ within Al₂O₃ layers grown on (001) In_{0.53}Ga_{0.47}As channel layers and the effects of hydrogen passivation of these defects.

The starting In_{0.53}Ga_{0.47}As surface was treated with 4 vol % NH₄OH(aq) solutions, followed by thermal desorption of residual As from the wet etching step at 380 °C prior to atomic layer deposition (ALD).⁵ Al₂O₃ films of different thicknesses, 2.4–16 nm, were prepared by ALD at 270 °C using trimethylaluminum and H₂O precursors. Film thicknesses were determined by ellipsometry, the readings of which were calibrated by cross-sectional transmission electron microscopy. For capacitance-voltage (CV) measurements, Pt top electrodes were deposited in an e-beam evaporator through a shadow mask. Postmetallization forming gas anneal (FGA) was carried out under forming gas (95%N₂+5%H₂) flowing at a rate of ~2 L/min at 400 °C for 50

min. The dielectric constant of the Al₂O₃ films was determined by linear fitting of the inverse of the maximum capacitance at accumulation at 800 kHz versus film thickness—to be 8.2 ± 0.5 and 6.8 ± 0.1 for the as-deposited and post-FGA films, respectively.⁶

First-principles calculations based on density functional theory were performed for κ -Al₂O₃; the κ phase was chosen because of the similarity of its density⁷ to that of amorphous Al₂O₃. We employed a hybrid-functional scheme⁸ as a way of overcoming the band-gap problem. We utilized projector-augmented-wave pseudopotentials⁹ and a plane-wave basis set with a 300 eV plane-wave cutoff as implemented in the VASP code.¹⁰ The percentage of Hartree–Fock exchange mixed into the hybrid functional was chosen to be 32% in order to optimally reproduce the experimental gaps of Al₂O₃ as well as InAs, GaAs, and InGaAs. The calculated Al₂O₃ gaps are 7.94 eV for the κ phase and 9.1 eV for the α phase, the latter in good agreement with experiment (8.8 eV, Ref. 11). There are no known experimental values for the band gap of κ -Al₂O₃. The band gap of the amorphous oxide has been measured to be 7.36 eV.¹² This is slightly lower than our calculated κ -Al₂O₃ band gap but this difference does not affect our conclusions.

To investigate the spatial distribution of fixed charge in as-deposited Al₂O₃ films on In_{0.53}Ga_{0.47}As, CV curves from MOS capacitors with different Al₂O₃ thicknesses were collected and are shown in Fig. 1(a). The thickness series exhibits a considerable negative shift of the flat-band voltage (V_{FB}) with increasing thickness, indicating the presence of net positive fixed charge in the as-deposited Al₂O₃. A closer examination of Fig. 1(a), however, reveals that the V_{FB} 's of thinner films (30, 45, 60 TMA/H₂O cycles) are more positive than the expected ideal V_{FB} (0.6–1.0 V, depending on the value of Pt work function and the exact substrate dopant concentration assumed in the estimation), indicating that the thinner films contain negative fixed charge. With increasing film thickness, V_{FB} becomes comparable to the ideal V_{FB} (after ~90 cycles of deposition), and then shifts to negative polarity for thicker ALD-Al₂O₃ layers. The observed

^{a)}Electronic mail: shinbh93@stanford.edu.

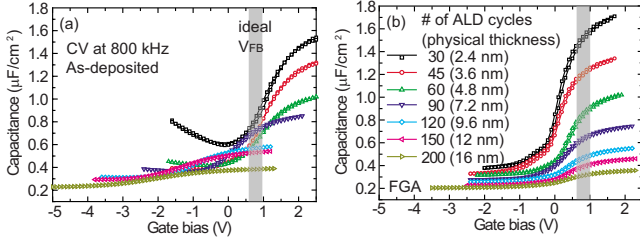


FIG. 1. (Color online) CV curves from Pt/ALD- Al_2O_3 /n- $\text{In}_{0.53}\text{Ga}_{0.47}\text{As}$ MOS capacitors with various Al_2O_3 layer thicknesses: (a) before, and (b) after postmetallization FGA at 400°C . Estimated range of ideal V_{FB} (0.6–1.0 V) is indicated by vertical gray bars in both figures.

thickness-dependence of V_{FB} can be rationalized if there is both *negative* fixed charge *near the interface* with the InGaAs channel and *positive bulk* fixed charge in the Al_2O_3 films.

This nonuniform distribution of fixed charge across the thickness of the Al_2O_3 films may result from a local variation in aluminum:oxygen stoichiometry. Table I lists the ratio of Al $2p$ to O $1s$ x-ray photoelectron spectroscopy (XPS) core level peak intensity for various Al_2O_3 layer thickness. A take-off angle (with respect to the sample surface) of 90° was used and, for the film thicknesses studied, peaks from the substrate (i.e., In, Ga, and As) were observed, meaning that the Al $2p$ and O $1s$ peaks include contributions from the entire thickness of each Al_2O_3 film. In previous work,⁵ we observed an interfacial In oxide from an ALD- Al_2O_3 /In_{0.53}Ga_{0.47}As sample which was prepared identically to those used in this study. However, any contribution from this interfacial In oxide to the total O $1s$ peak intensity is negligible because its areal coverage is only $\sim 12\%$ and it is buried under an Al_2O_3 layer which attenuates most of O $1s$ photoelectrons from the interfacial In oxide. A clear trend of increasing Al:O atomic ratio with increasing film thickness is evident, and this suggests that the films are O-rich near the interface and become progressively more Al-rich farther away from the interface. Therefore, it appears that the sign of fixed charge is correlated with the local stoichiometry of the films, such that negative fixed charge exists within O-rich regions near the interface and positive fixed charge within Al-rich regions away from the interface.

The effect of local variations in stoichiometry was investigated using first-principles calculations as described above. In an amorphous oxide, Al deficiency may predominantly manifest itself in the form of oxygen dangling bonds (DBs), and O deficiency in the form of Al DBs. We have therefore performed a study of the atomic and electronic structure of DBs in Al_2O_3 , using geometries previously applied to group-IV semiconductors.¹³ The DBs were studied in an 80-atom bulk κ - Al_2O_3 supercell with occupancies of zero, one, and two electrons, as well as with hydrogen passivating them. As shown in Fig. 2, the oxygen DB gives rise to charge-state transition levels at -0.83 eV and 0.61 eV above the valence-band maximum (VBM) of Al_2O_3 , while the Al DB produces levels at 5.12 and 5.35 eV above the VBM. Therefore, using a VB offset of 2.8 eV between

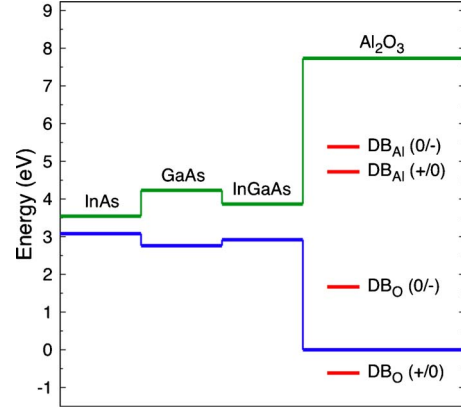


FIG. 2. (Color online) Band alignment between Al_2O_3 and relevant semiconductors, and position of charge-state transition levels for dangling bonds in the oxide.

In_{0.53}Ga_{0.47}As and Al_2O_3 ,¹⁴ we conclude that O DBs will always be below the Fermi level and thus negatively charged, while Al DBs will be positively charged. This is consistent with the experimental findings that O-rich regions have fixed negative charge, while Al-rich regions have fixed positive charge.

We have also studied hydrogen passivation by comparing calculated total energies of the passivated DBs with unpassivated DBs plus interstitial hydrogen. The resulting binding energies are 1.3 eV for O–H and 1.4 eV for Al–H, indicative of stable passivation. Hydrogen passivation neutralizes the DBs, i.e., the O–H and Al–H bonds occur exclusively in the neutral charge state over the relevant range of Fermi levels. We note that complete neutralization may not be possible in the case of vacancies that contain multiple dangling bonds, although addition of hydrogen will still reduce the amount of fixed charge per vacancy.

The prediction that hydrogen can effectively passivate DBs in the oxide can be tested by comparison to experimental data. CV curves from the samples, which received FGA at 400°C after electrode deposition, are shown in Fig. 1(b). The flat band voltage, which exhibited a wide variation depending on the Al_2O_3 layer thickness of the as-deposited films, was shifted in all cases to a value very close to the ideal V_{FB} after the FGA, suggesting that annealing in hydrogen can compensate most of the positive bulk fixed charge and the negative interfacial fixed charge. In addition to the compensation of the fixed charge in Al_2O_3 by the FGA, we notice significant improvements in the CV characteristics—such as a decrease in frequency dispersion in depletion and accumulation, and a decrease in CV stretch-out, indicative of passivation of interface states by the FGA [compare Figs. 3(a) and 3(b)]. We would like to point out that enhancement of high- k /In_{0.53}Ga_{0.47}As interface quality by FGA is not limited to an Al_2O_3 /In_{0.53}Ga_{0.47}As interface; the reduction in interface state density has been observed from an ALD- HfO_2 /n- $\text{In}_{0.53}\text{Ga}_{0.47}\text{As}$ interface after postmetallization FGA at 325°C .¹⁵

TABLE I. Ratio of Al $2p$ to O $1s$ XPS peak intensity for different Al_2O_3 film thicknesses.

Al_2O_3 film thickness (nm)	2.4	2.8	3.6	4.8
Ratio: Al $2p$ peak intensity to O $1s$ peak intensity	0.141	0.145	0.154	0.157

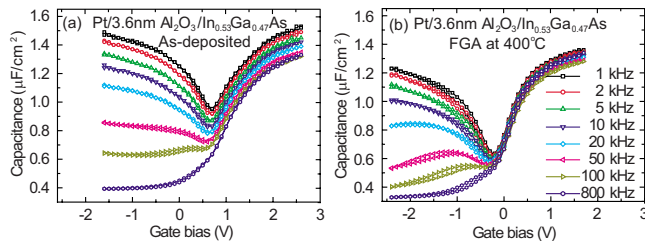


FIG. 3. (Color online) Comparison of ac frequency-dependent CV curves from (a) as-deposited and (b) forming gas annealed Pt/ALD- $\text{Al}_2\text{O}_3/\text{In}_{0.53}\text{Ga}_{0.47}\text{As}$ MOS capacitors. Bidirectional gate bias sweep (inversion \Rightarrow accumulation \Rightarrow inversion) was used.

The authors acknowledge support from SRC (NonClassical CMOS Center Task No. 1437.003 and Grant No. 2009-VJ-1867) and Intel Corp. RDL acknowledges support from Irish Fulbright Commission and Fulbright USA.

¹B. Shin, D. Choi, J. S. Harris, and P. C. McIntyre, *Appl. Phys. Lett.* **93**, 052911 (2008); M. Milojevic, F. S. Aguirre-Tostado, C. L. Hinkle, H. C. Kim, E. M. Vogel, J. Kim, and R. M. Wallace, *ibid.* **93**, 202902 (2008); N. V. Nguyen, O. A. Kirillov, W. Jiang, W. Wang, J. S. Suehle, P. D. Ye, Y. Xuan, N. Goel, K. W. Choi, W. Tsai, and S. Sayan, *ibid.* **93**, 082105 (2008); H. C. Chiu, L. T. Tung, Y. H. Chang, Y. J. Lee, C. C. Chang, J. Kwo, and M. Hong, *ibid.* **93**, 202903 (2008); V. V. Afanas'ev, M. Badylevich, A. Stesmans, G. Brammertz, A. Delabie, S. Sionke, A. O'Mahony, I. M. Povey, M. E. Pemble, E. O'Connor, P. K. Hurley, and S. B. Newcomb, *ibid.* **93**, 212104 (2008); Y. Oshima, Y. Sun, D. Kuzum, T. Sugawara, K. C. Saraswat, P. Pianetta, and P. C. McIntyre, *J. Electrochem. Soc.* **155**, G304 (2008).

²S. Barraud, O. Bonno, and M. Casse, *J. Appl. Phys.* **104**, 073725 (2008); J. P. Locquet, C. Marchiori, M. Sousa, J. Fompeyrine, and J. W. Seo, *ibid.*

100, 051610 (2006).

³G. D. Wilk, R. M. Wallace, and J. M. Anthony, *J. Appl. Phys.* **89**, 5243 (2001).

⁴The term, "fixed charge" in this article should be distinguished from conventional interface states whose charging state varies depending on the position of the semiconductor Fermi level.

⁵B. Shin, J. Cagnon, R. D. Long, P. K. Hurley, S. Stemmer, and P. C. McIntyre, *Electrochem. Solid-State Lett.* **12**, G40 (2009).

⁶There is an apparent decrease in the dielectric constant after the FGA, which we attribute to the incorporation of hydroxyl groups as revealed by the comparison of the O 1s XPS spectra before and after the FGA. A similar phenomenon (an inverse correlation between dielectric constant of ALD- Al_2O_3 and H content) was observed by other group. See, M. D. Groner, J. W. Elam, F. H. Fabreguette, and S. M. George *Thin Solid Films* **413**, 186 (2002).

⁷D. R. Jennison, P. A. Schultz, and J. P. Sullivan, *Phys. Rev. B* **69**, 041405 (2004).

⁸J. Heyd, G. E. Scuseria, and M. Ernzerhof, *J. Chem. Phys.* **118**, 8207 (2003); M. Marsman, J. Paier, A. Stroppa, and G. Kresse, *J. Phys.: Condens. Matter* **20**, 064201 (2008).

⁹P. E. Blöchl, *Phys. Rev. B* **50**, 17953 (1994).

¹⁰G. Kresse and J. Furthmüller, *Phys. Rev. B* **54**, 11169 (1996); *Comput. Mater. Sci.* **6**, 15 (1996); G. Kresse and D. Joubert, *Phys. Rev. B* **59**, 1758 (1999).

¹¹R. A. French, *J. Am. Ceram. Soc.* **73**, 477 (1990).

¹²J. Price, G. Bersuker, and P. S. Lysaght, *J. Vac. Sci. Technol. B* **27**, 310 (2009).

¹³C. G. Van de Walle and R. A. Street, *Phys. Rev. B* **49**, 14766 (1994); J. R. Weber, A. Janotti, P. Rinke, and C. G. Van de Walle, *Appl. Phys. Lett.* **91**, 142101 (2007).

¹⁴J. R. Weber, A. Janotti, and C. G. Van de Walle, *Microelectron. Eng.* **86**, 1756 (2009).

¹⁵E. O'Connor, S. Monaghan, R. D. Long, A. O'Mahony, I. M. Povey, K. Cherkaoui, M. E. Pemble, G. Brammertz, M. Heyns, S. B. Newcomb, V. V. Afanas'ev, and P. K. Hurley, *Appl. Phys. Lett.* **94**, 102902 (2009).